J|A|C|S

A R T I C L E S

An X-ray Diffraction and MAS NMR Study of the Thermal Expansion Properties of Calcined Siliceous Ferrierite

Ivor Bull,[†] Philip Lightfoot,[†] Luis A. Villaescusa,[†] Lucy M. Bull,[‡]
Richard K. B. Gover,[§] John S. O. Evans,[§] and Russell E. Morris*,[†]

*Contribution from the School of Chemistry, University of St. Andrews, The Purdie Building,
North Haugh, St. Andrews, Fife KY16 9ST, U.K., Catalyst Group,
Chevron Texaco Energy Research and Technology Company, 100 Chevron Way, P.O. Box 1627,
Richmond, California 94802-0627, and Department of Chemistry,
University Science Laboratories, University of Durham, South Road, Durham DH1 3LE, U.K.*

Received November 6, 2002; E-mail: rem1@st-and.ac.uk

Abstract: Powder and single-crystal X-ray diffraction, combined with MAS NMR measurements, has been used to study the thermal expansion of siliceous zeolite ferrierite as it approaches a second-order displacive phase transition from a low-symmetry (*Pnnm*) to a high-symmetry (*Immm*) structure. Below the transition temperature, ferrierite exhibits positive thermal expansivity. However, above the transition temperature a significant change in thermal behavior is seen, and ferrierite becomes a negative thermal expansion material. Accurate variable-temperature single-crystal X-ray diffraction measurements confirm the transition temperature and allow the changes in average atomic position to be followed with temperature. The results from the single-crystal X-ray diffraction study can be correlated with ^{29}Si MAS NMR chemical shifts for the low-temperature phase. At low temperatures the results show that the positive thermal expansivity is driven by an overall increase in Si—Si distances related to an increase in Si—O—Si bond angles. However, in the high-temperature phase the Si—O—Si angles are approximately invariant with temperature, and the negative thermal expansion in this case is caused by transverse vibrations of the Si—O—Si units.

Introduction

Most materials expand when exposed to an increase in temperature. However, there is a significant group of materials that actually contract as the temperature is raised. These materials are said to show negative thermal expansion (NTE).[1] The thermal behavior of zeolites has become of interest since it was recognized that many such materials exhibit NTE. It is clear now that a significant number of purely siliceous zeolites and aluminum phosphates show this effect,[2] and that materials such as AlPO-17 have some of the most negative linear coefficients of thermal expansion of any materials known.[3] In previous work some of us have used neutron and powder X-ray diffraction to show that siliceous zeolites with the framework structures MWW, ITE, STT, CHA, IFR, ISV, and STF all show NTE.[2a,4,5] Powder X-ray diffraction gives good information on changes in the unit cells. However, the most powerful technique to study how the average atomic positions change during this process is undoubtedly single-crystal X-ray diffraction (SCXRD). We have used SCXRD to understand more fully the changes in the structure of zeolite IFR as it contracted with temperature.[6] This allowed us to identify the regions in the structure that were important in the process, and to use this information to show that the thermal behavior of a zeolite can be correlated with its structural features, and in particular how "dense" the walls of the zeolite channels are.

Ferrierite (FER) is a well-known aluminosilicate zeolite mineral[7] that can also be prepared readily by both aqueous[8] and nonaqueous routes.[9] An understanding of the structure and properties of FER remains important because of its role as a catalyst in commercial reactions. For example, it is important in the petrochemical industry, where it has been used as a shape-selective catalyst for the production of isobutene.[10] The reaction takes place at elevated temperatures, so it is also important to study thoroughly the thermal behavior of these materials. The

* Address correspondence to this author. Phone: +44 (0) 1334 463818.
† University of St. Andrews.
‡ Chevron Texaco Energy Research and Technology Co.
§ University of Durham.

 (1) (a) Evans, J. S. O *J. Chem. Soc., Dalton. Trans*. **1999**, 3317. (b) Korthuis, V.; Khosrovani, N.; Sleight, A. W.; Roberts, N.; Dupree R.; Warren, W. W. *Chem. Mater*. **1995**, *7*, 412. (c) Evans, J. S. O.; Mary, T. A.; Vogt, T.; Subramanian, M. A.; Sleight, A. W. *Chem. Mater*. **1996**, *8*, 2809. (d) Evans, J. S. O.; Mary, T. A.; Sleight, A. W. *J. Solid State Chem*. **1998**, *137*, 148.
 (2) (a) Lightfoot, P.; Woodcock, D. A.; Maple, M. J.; Villaescusa, L. A.; Wright, P. A. *J. Mater. Chem*. **2001**, *11*, 212. (b) Park, S. H.; Grosse-Kunstleve, R. W.; Graetsch H.; Gies, H. *Stud. Surf. Sci. Catal*. **1997**, *105*, 1989. (c) Couves, J. W.; Jones, R. H.; Parker, S. C.; Tschaufeser P.; Catlow, C. R. A. *J. Phys.: Condens. Matter* **1993**, *5*, 329. (d) Colantuano, A.; Dal Vecchio, S.; Mascolo G.; Pansini, M. *Thermochim. Acta* **1997**, *29*, 659.
 (3) Attfield, M. P.; Sleight, A. W. *Chem. Mater*. **1998**, *10*, 2013.
 (4) Woodcock, D. A.; Lightfoot, P.; Wright, P. A.; Villaescusa, L. A.; Diaz-Cabanas, M.-J.; Camblor M. A. *J. Mater. Chem*. **1999**, *9*, 349.
 (5) Woodcock, D. A.; Lightfoot, P.; Wright, P. A.; Villaescusa, L. A.; Diaz-Cabanas, M.-J.; Camblor M.-J.; Engberg, D. *Chem. Mater*. **1999**, *11*, 2508.
 (6) Villaescusa, L. A.; Lightfoot, P.; Teat, S. J.; Morris, R. E. *J. Am. Chem. Soc*. **2001**, *123*, 5453.
 (7) Wise, W. S.; Tschernich, R. W. *Am. Mineral*. **1976**, *61*, 60.
 (8) Gies, H.; Gunawardane, R. P. *Zeolites* **1987**, *7*, 442.
 (9) Kuperman, A.; Nadimi, S.; Oliver, S.; Ozin, G. A.; Garces J. M.; Olken, M. M. *Nature* **1993**, *365*, 239.
 (10) Yamahara, K.; Okazaki, K.; Kawamura, K. *Catal. Today* **1995**, *23*, 397.
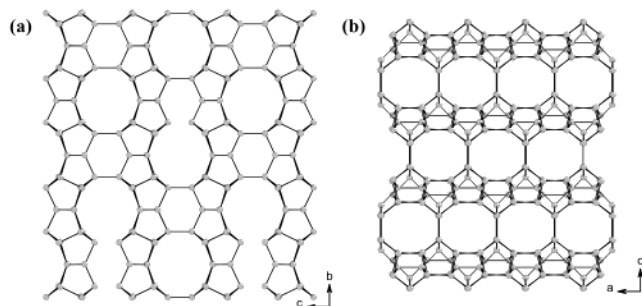
Figure 1. Framework topology of ferrierite. The silicons are shown in gray, and the oxygens have been removed for clarity. (a) shows the rows of 10MR channels joined by 6MR channels viewed down the *a* axis. (b) shows the rows of 8MR channels viewed down the *b* axis.

room-temperature structure of FER is dependent on the framework and extraframework composition of the material. For natural aluminosilicate zeolite FER the structure solution was first accomplished in space group *Immm*.[7] Recently Yokomori et al. have described another natural aluminum-containing ferrierite in *I*222 as containing five crystallographically unique silicon atoms and none of the 180° bond constraints[11] required by the higher symmetry *Immm* space group. However, studies of purely siliceous FER conclusively showed that the room-temperature structure was better described, on the basis of joint powder synchrotron X-ray and neutron studies, in the lower symmetry *Pnnm* space group for this particular material.[12] This has been confirmed by further single-crystal studies on both the calcined and as-made materials.[13,14] However, there has long been speculation that a phase transition may occur at higher temperatures, but to our knowledge no such phase transition has been definitively shown prior to this current work.

In this paper we report just such a phase transition. In addition, we report powder and single-crystal X-ray diffraction studies on the thermal expansion behavior of the material, with strong positive thermal expansion behavior in the low-temperature form and strong negative thermal expansion in its high-temperature form. The results of the diffraction experiments for the low-temperature phase can be correlated with [29]Si chemical shift values resulting from MAS NMR studies. Bull and co-workers have shown elegantly that the correlation of crystallographically derived structural features with NMR chemical shifts requires the very highest quality data, with even the best joint refinements against X-ray and neutron powder diffraction data not yielding results as accurate as those from single-crystal X-ray diffraction studies.[15]

The crystal structure of ferrierite is built up of rings of five corner-shared SiO$_4$ tetrahedra (known as five-membered rings or 5MRs) building units, which form layers in the *ab* plane. The layers are connected by a single Si−O−Si bridge, and form a matrix of 10MR channels running parallel to the *c* axis, which are intersected by 8MR channels running parallel to the *b* axis (see Figure 1). Six-membered rings connect the 10MRs along the *c* axis direction.

There are a number of phase transitions known for zeolites, perhaps the most famous being in zeolite ZSM-5 (MFI). This material, which is extremely well utilized in industry for catalytic transformations, has a low-temperature monoclinic form and a high-temperature orthorhombic form, which can easily be identified by their ^{29}Si MAS NMR spectra. Gies and co-workers[2b] have shown by means of Guiner X-ray studies that MFI expands in its low-temperature form with temperature but contracts in its high-temperature form. However, no structural studies have been carried out on any zeolites to understand the differences between the two types of behavior. The cause of NTE in microporous materials is undoubtedly the transverse vibrations of the two connected oxygen atoms. This is because a transverse vibration of a Si−O−Si bond inevitably reduces the Si−Si distance if the constituent Si−O bond distances remain approximately constant. These vibrations can take place in a correlated fashion in phonon modes that do not change the Si−O distances or O−Si−O bond angles in the SiO$_4$ tetrahedra themselves, but do excite transverse Si−O−Si vibrations. These modes are called floppy or rigid unit modes (RUMs).[1a,16] Modes that produce only very slight distortions of the tetrahedra are called quasi-rigid unit modes (qRUMs). However, comparison of calculation with experiment shows that the presence of RUMs is not enough in itself to determine whether NTE will occur, as there are some materials that show NTE but have no RUMs (and vice versa). There is a great need for accurate experimental studies that can in the future be compared with theory to add insight into this fascinating and potentially useful effect. X-ray diffraction gives accurate and precise information on how such vibrations change the positions of the atoms in the structure, averaged over time and space, and give a valuable benchmark whereby the results of calculations based on rigid unit modes can be validated. In this paper we report variable-temperature X-ray diffraction and NMR studies aimed at elucidating the properties of zeolite FER in the low- and high-temperature phases.

Experimental Section

Synthesis. Samples of purely siliceous FER were prepared from fluoride-containing media using pyridine as a templating (structure-directing) agent to give as-made materials of formula Si$_{36}$O$_{72}$·2C$_5$H$_5$N. A 6.08 g sample of TEOS (tetraethyl orthosilicate) was hydrolyzed in 52.84 g of an aqueous solution of *N,N*-dimethyl-6-azonium-1,3,3-trimethylbicyclo[3.2.1]octane (DMABO$^+$) in hydroxide form, which corresponds to 0.28 mmol of DMABO$^+$/g of solution. The solution was reduced to a gel by evaporating all of the ethanol produced (∼4.4 g) and most of the water (∼48 g). A 0.61 g sample of HF was added dropwise with stirring by hand. The resultant paste was transferred to Teflon-lined acid digestion bombs (23 mL, Parr), and pyridine (Pyr) was added according to the overall composition 0.5 DMABO−OH: 0.5 HF:1.5 H$_2$O:SiO$_2$:0.8 Py. The mixture was heated under static conditions at 423 K for 38 days. It was then removed from the furnace and quenched. The ferrierite was then washed with deionized water and dried at 353 K. The products contained small crystals (approximately 50 μm × 50 μm × 10 μm) that were suitable for microcrystal X-ray diffraction studies. The pyridine and fluoride ions were removed by carefully heating the crystals at 1 deg min^{-1} to 873 K under flowing oxygen. The integrity of the crystals remained intact after the calcination. Thermogravimmetric analysis of the calcined material indicates that the sample gains negligible weight on exposure

(11) Yokomori, Y.; Wachsmuth, J.; Nishi, K. *Microporous Mesoporous Mater.* **2001**, *50*, 137.
(12) Lewis, J. E.; Freyhardt, C. C.; Davis, M. E. *J. Phys. Chem.* **1996**, *100*, 5039.
(13) Morris, R. E.; Weigel, S. J.; Henson, N. J.; Bull, L. M.; Janicke, M. T.; Chmelka, B. F.; Cheetham, A. K. *J. Am. Chem. Soc.* **1994**, *116*, 11849.
(14) Weigel, S. J.; Gabriel, J.; Guttierez Puebla, E.; Monge Bravo, A.; Henson, N. J.; Bull, L. M.; Cheetham, A. K. *J. Am. Chem. Soc.* **1996**, *118*, 2427.
(15) Bull, L. M.; Bussemer, B.; Anupold, T.; Reinhold: A.; Samoson, A.; Sauer, J.; Cheetham, A. K.; Dupree, R. *J. Am. Chem. Soc.* **2000**, *122*, 4948.

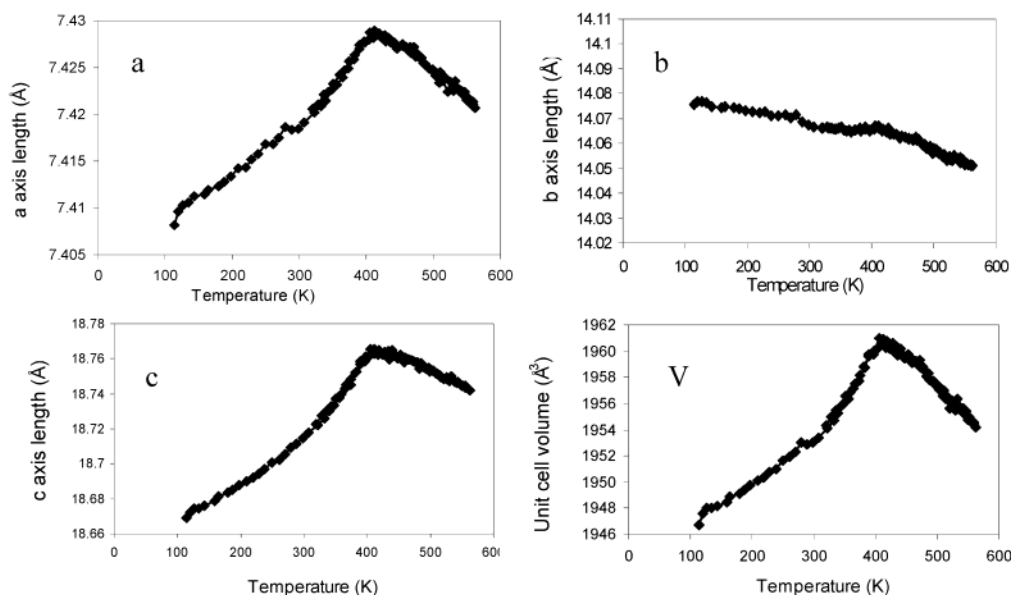(16) Bieniok, A.; Hammonds, K. D. *Microporous Mesoporous Mater.* **1998**, *25*, 193.

Figure 2. Thermal evolution of unit cell parameters for siliceous ferrierite. The inflection at the phase transition can be clearly seen in graphs a, c, and V, but there is also a change of behavior in graph b. Data collected from 110 to 560 K on warming and from 360 to 300 K on cooling are shown.

to the air and therefore does not adsorb sufficient water to affect the results of the experiment.

Powder X-ray Diffraction. Variable-temperature powder X-ray diffraction experiments were carried out using a Bruker d8 X-ray diffractometer (Cu Kα$_1$ radiation) to study the thermal behavior. Samples of calcined ferrierite were ground together with a small amount of Al$_2$O$_3$ and sprinkled onto an aluminum plate inside a TTK450 cryofurnace. Data were collected from 5° to 90° in 2θ in steps of 0.0144° from 110 up to 560 K and then back down to 300 K in 10 K intervals under a dynamic vacuum. The experiment took approximately 60 h. The temperature of the furnace was calibrated by following the thermal expansion of both the Al$_2$O$_3$ internal standard and the Al sample holder. The unit cell data were extracted from each of the runs using full three-phase Rietveld refinement.

Single-Crystal X-ray Diffraction. Single-crystal X-ray diffraction experiments were carried out at the CCLRC Synchrotron Radiation Source, Daresbury Laboratories, U.K., using an X-ray diffractometer equipped with a CCD detector. Thirteen data sets were collected between 133 and 513 K. The low-temperature data (133−300 K) were collected using an Oxford liquid nitrogen cryostream, and the high-temperature data (333−513 K) were collected using a thermostream hot air heater. While the unit cells derived from these data agreed in their trends with those from the powder data, there were some differences in absolute values obtained between the two methods. However, it is clear that the unit cell dimensions measured from single-crystal X-ray diffraction are inferior when compared to those from powder diffraction. The reasons for this include the uncertainty in the wavelength of the synchrotron X-rays, the greater number of corrections necessary for the accurate measurement of diffraction spot positions, and the fact that the mounting of the crystal is more susceptible to changes in temperature as the mounting position changes during orientation of the crystal. Most importantly, the powder X-ray diffraction experiment involves two internal standards, and is therefore a much more reliable measurement.

Differential Scanning Calorimetry. The enthalpy and temperature changes during the phase transition were determined using a Perkin-Elmer DSC7 differential scanning calorimeter. Data were collected for heating and cooling runs in the temperature range of 123−573 K.

Magic Angle Spinning NMR. The ^{29}Si NMR spectra of calcined ferrierite were collected on a Bruker DSX 400 (CRMHT Orleans, with Dominique Massiot and Pierre Florian) using a 4 mm Bruker MAS probe. The sample was spun at 4 kHz, and data were collected using

a 90° pulse length of 3.5 μs and a relaxation delay of 30 s. Typically 32 scans were acquired. The spectra are referenced to TMS at 0 ppm. Temperatures were calibrated using the ^{207}Pb temperature-dependent NMR shift of Pb(NO$_3$)$_3$. The samples were left for 20 min at each temperature to reach temperature equilibrium before the ^{29}Si or ^{207}Pb spectra were collected.

Results and Discussion

Differential scanning calorimetry (DSC) shows a second-order phase transition at about 400 K. The associated enthalpy change of the transition is 24.71 J g^{-1}. The powder X-ray diffraction studies (Figure 2) clearly show a sharp maximum in the evolution of unit cell volume with temperature, consistent with a phase transition just above 400 K. Below this temperature siliceous ferrierite exhibits positive thermal expansion (i.e., its total unit cell volume expands with increasing temperature) with an average coefficient of volume expansion of approximately 25.1 × 10^{-6} K^{-1} [150−400 K].[17] However, it does so anisotropically, with the *a* and *c* unit cell axes both expanding up to the phase transition temperature (α$_a$ = 8.1 × 10^{-6} K^{-1} [150−400 K] and α$_c$ = 16.1 × 10^{-6} K^{-1} [150−400 K], where α$_x$ = is the coefficient of linear expansion in direction *x*) while the *b* unit cell axis contracts with increasing temperature (α$_b$ = −2.8 × 10^{-6} K^{-1} [150−400 K]). Anisotropic thermal expansion (whether positive or negative) is not unusual in zeolites and is of course related to different structural connectivity and rigidity in the three directions.[6] At temperatures higher than the transition temperature all three crystallographic axes contract in length, leading to negative thermal expansion with an average coefficient of volume expansion of −24.2 × 10^{-6} K^{-1} [420−560 K], and coefficients of linear expansion of α$_a$ = −6.7 × 10^{-6} K^{-1} [420−560 K], α$_b$ = −7.1 × 10^{-6} K^{-1} [420−560 K], and α$_c$ = −10.6 × 10^{-6} K^{-1} [420−560 K]. The change in unit cell parameters is reversible; there is no significant hysteresis on cooling the sample.

The single-crystal refinements were carried out in both *Pnnm*

---

(17) Defined as Δ*V*/*V*Δ*T*, where *V* is the volume and *T* is temperature. Some papers quote the average coefficient of linear expansion, which is equal to one-third of our value.
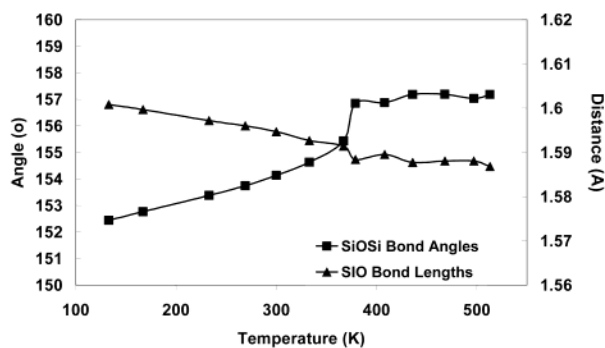
Figure 3. Evolution of average Si−O bond distances and Si−O−Si bond angles with temperature.

and *Immm* over the temperature range of 133−513 K. Below the transition temperature refinement in *Pnnm* gives the better results. This is confirmed by the presence in the data set of reflections that break the *I*-centering systematic absence conditions. At and above the transition temperature the *Immm* refinement yields the lower *R* values, although, since *Pnnm* is a subgroup of *Immm*, the difference is small. In addition, the relative intensity of those reflections that break the *I*-centering decrease steadily with increasing temperature until above 400 K they are all absent from the data set. Unfortunately, it is also clear that the quality of the refinements above 400 K decreases somewhat. Heating to the higher temperatures resulted in some softening of the glue and glass used to mount the crystals, which led to difficulty in centering the crystal in the X-ray beam and in keeping it centered throughout the data collection. Similar problems have been seen in previous variable-temperature single-crystal X-ray diffraction experiments.[6] Both these effects resulted in the very-high-temperature refinements being of slightly less precision compared to those in the low-temperature range. However, this principally affects the measurement of reflection positions, and therefore the calculation of the unit cells. The integration of intensities in the SCXRD experiment is less seriously affected, and accurate intensities can be extracted even from the high-temperature data. The atomic positions, and hence calculated bond distances and angles, are reliable even for the high-temperature data (although their precision is worse) and follow the same trends as those from the better refinements (see below).

From the SCXRD experiments there seems to be no significant distortion of the SiO4 tetrahedra with temperature, consistent with them being relatively rigid units, hinged by more flexible Si−O−Si linkages. However, Figure 3 shows that there are two competing processes occurring. All the Si−O bond distances seem to decrease with increasing temperature. This apparent shortening of bond distances is a well-known feature of X-ray diffraction experiments and is caused by libration. This shows that there are transverse vibrations active at these temperatures. As described above, these vibrations are volume reducing. The average Si−O−Si angles, however, show a marked increase up to the phase transition temperature. An increase in the average Si−O−Si bond angle is a volume-increasing structural change as this necessarily increases the silicon−silicon interatomic distances in the structure. So in the low-temperature form of FER there are at least two competing processes: a volume-increasing distortion of the Si−O−Si angles and a volume-reducing excitation of transverse vibrations.
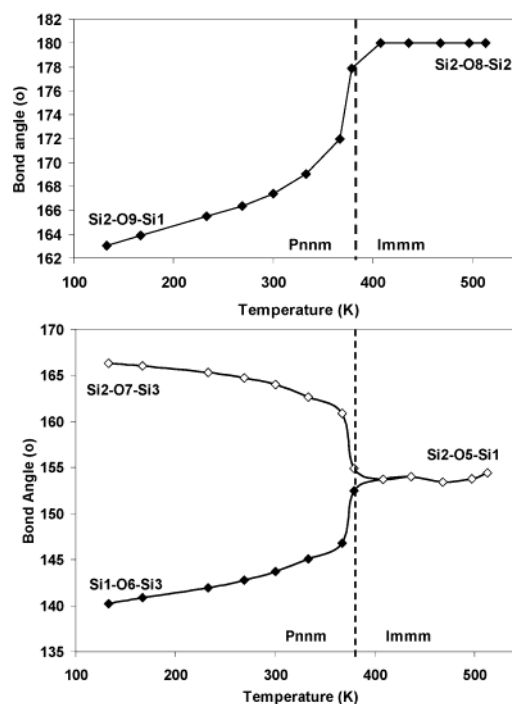

Figure 4. (Top) The value of the S2−O9−Si1 (*Pnnm*) bond angle approaches 180° as the temperature approaches the phase transition temperature. The equivalent bond angle in the *Immm* description is constrained to be 180° by symmetry. (Bottom) Symmetry-inequivalent bond angles in the low-temperature *Pnnm* refinement steadily move toward their average values as the phase transition temperature is approached. The estimated standard deviations for the bond angles are in the range 0.1− 0.2° below the phase transition, rising to 0.3−0.6° above the phase transition.

Above the phase transition, however, there are no longer any significant changes in average Si−O−Si bond angles, while the librations are still present as the apparent Si−O distances continue to decrease.

The changes in Si−O distances and Si−O−Si angles are consistent with the volume changes seen in the PXRD experiment. Below 400 K the *Pnnm* phase exhibits positive thermal expansivity, so the changes in Si−O−Si angles must dominate. In the *Immm* phase, there are no longer any significant bond angle changes and the transverse vibrational modes dominate, leading to an overall decrease in volume in this phase. However, in both cases the thermal expansion/contraction is anisotropic, and to explain this, the changes in individual atomic positions and the resulting effect on the overall structure must be studied (see below).

The high-temperature *Immm* symmetry constrains one of the Si−O−Si angles to 180°. There are also some subtle changes to the shape of the pore openings that will be discussed below. Bond angles calculated from the average atomic positions clearly show that the structure slowly begins to move toward the *Immm* structure below the transition temperature. For example, Figure 4 shows how the Si2−O9−Si1 bond angle in the low-temperature *Pnnm* structure approaches the value of 180° as the temperature nears that where the phase transition takes place. In the *Immm* refinement above the transition temperature the equivalent angle is constrained to be 180° by the symmetry of the space group. Note that, because of the different numbers of crystallographically independent atoms in the two space groups, the numbering schemes in the two descriptions are necessarily different.
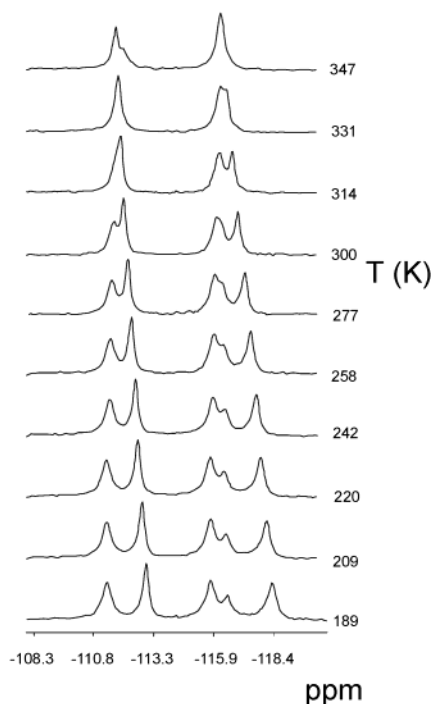
Figure 5. Temperature dependence of ^{29}Si NMR spectra for purely siliceous ferrierite.

Figure 6. (Top) Average of $\cos(\alpha)/(\cos(\alpha) - 1)$ (where α is the Si–O–Si bond angle around each silicon atom) versus temperature for the five independent silicon atoms in the low-temperature form of ferrierite and the four silicon atoms of the high-temperature form and (bottom) variation of the ^{29}Si chemical shift for the five silicon atoms of the low-temperature form of ferrierite.

Because some of the crystallographically independent atoms in the *Pnnm* description of the structure become equivalent by symmetry in the *Immm* description, then some bond angles also become equivalent. Figure 4 also shows how the value of bond angles that are nonequivalent (and often quite different in magnitude) approach their average value as the transition temperature approaches, and after the transition any changes in the bond angles are much less significant.

Silicon-29 magic angle spinning NMR spectroscopy is a powerful method of characterizing the local structure around the silicon atoms in the structure of a zeolite, yielding information on the number of crystallographic sites present, their relative proportions, their connectivity, and the presence of any impurity/dopant elements. Variable-temperature ^{29}Si MAS NMR spectra collected from 189 to 347 K showed significant changes in the chemical shifts of the various silicon sites (Figure 5). The five low-temperature resonances that are clearly visible have been previously assigned to the five independent silicon atoms in the *Pnnm* description of the ferrierite structure using room-temperature INADEQUATE experiments.[13] As temperature increases the resonances shift, the two low-field resonances seeming to coalesce at ∼∠112 ppm and the three high-field resonances coalescing at ∼116 ppm. At first sight it is tempting to suggest that the fewer resolved peaks in the spectra above 314 K indicate the onset of the phase transition, yielding fewer resonances because of the decreased number of silicon sites in the high-temperature phase. However, it should be noted that due to instrumental limitations we were not able to collect spectra above 347 K, which is still below the transition temperature. In addition, the two silicon atoms Si1 and Si2 that become equivalent in the high-temperature phase have been unambiguously assigned to the lowest and highest field resonances, respectively (at 189 K Si1 is at 111.4 ppm and Si2 is at −118.3 ppm). These two resonances do not coalesce in the
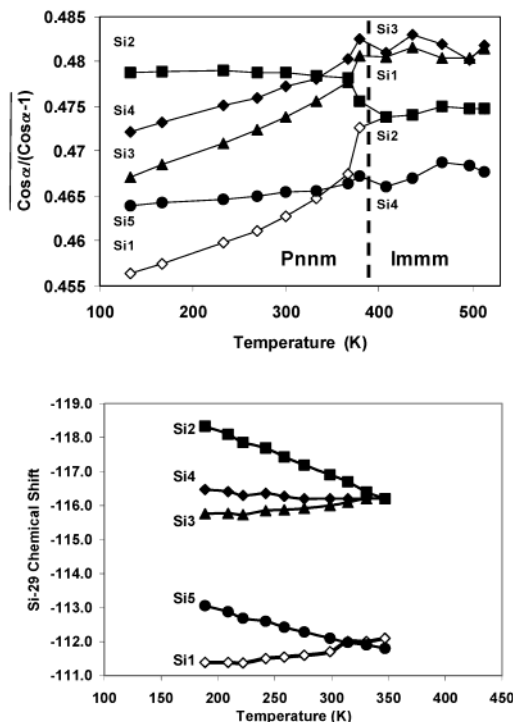
observed spectra, indicating that we are still below the phase transition temperature.

Fyfe[18] and Dupree[19] have shown that the ^{29}Si chemical shift in MAS NMR experiments can be correlated with certain geometrical features of a zeolite structure. For example, in silicalite, the purely siliceous zeolite with the MFI (ZSM-5) framework structure, the chemical shifts of the individual silicon sites correlate extremely well with a simple function of the cosine of the average of the four Si–O–Si bond angles around the particular silicon atom. This correlation has also been shown to hold well for ferierrite in a number of publications,[13,14,16] and the assignment of the resonances made using this correlation is consistent with those made using the INADEQUATE experiments.[13] From the results of the single-crystal diffraction experiments it is straightforward to calculate the average of $\cos(\alpha)/(\cos(\alpha) - 1)$, where α is the Si–O–Si bond angle around each of the silicon sites, as a function of temperature. This function is plotted in Figure 6. Comparing this plot with that of the individual chemical shifts as a function of temperature, we see that the two graphs show the same form. At low temperatures the $\cos(\alpha)/(\cos(\alpha) - 1)$ function shows the five silicon atoms having significantly different values, indicating that their chemical shifts would be well separated, and that the NMR spectrum would yield five well-resolved lines. This is indeed the case. As temperature increases the behavior of the $\cos(\alpha)/(\cos(\alpha) - 1)$ curves resembles that of the chemical shift curves. We plainly see that in both cases the behavior splits

(18) Fyfe, C. A.; Feng, Y.; Grondey, H. *Microporous Mater.* **1993**, *1*, 393.
(19) Dupree, R.; Cohn, S.; Henderson, C. M. B.; Bell, A. M. T. In *Nuclear Magnetic Shielding and Molecular Structure*; Tossell, J. A., Ed.; NATO ASI Series, Vol. 386; Kluwer Academic: Dordrecht, The Netherlands, 1992; p 421.
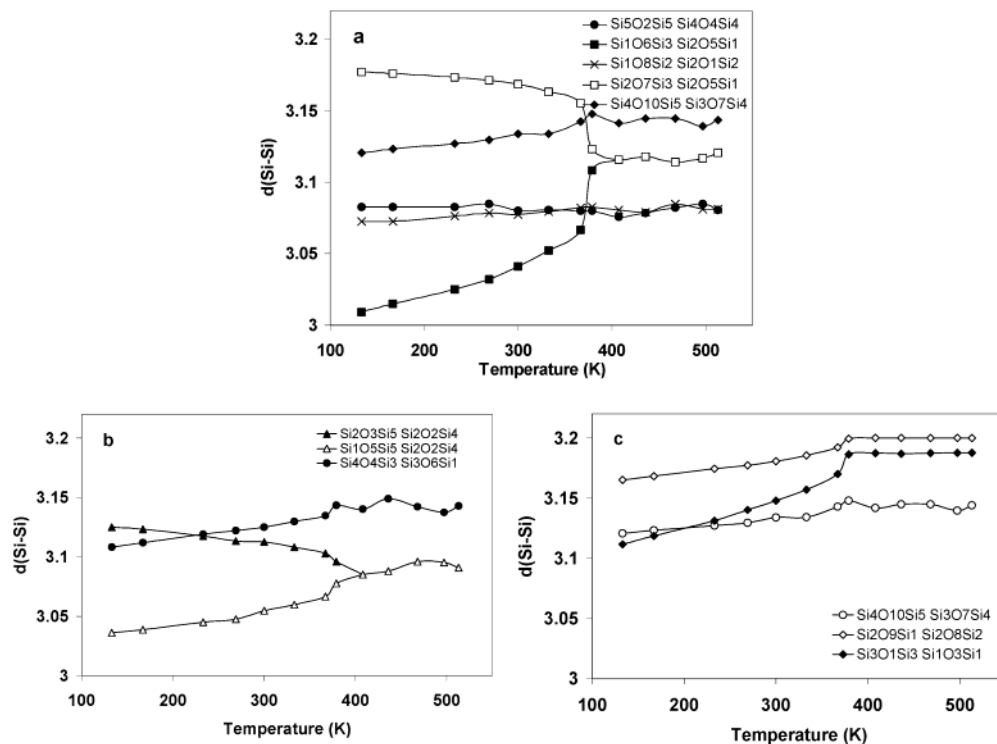
Figure 7. Calculated Si(O)Si interatomic distances (Å) for all Si−O−Si linkages in the FER structure as a function of temperature. The value of the interatomic distance is calculated from the equation $d(\text{Si}-\text{Si}) = 2l \sin(\theta/2)$, where l is the average of the two Si−O bond distances and θ is the Si−O−Si bond angle. This shows how changes in the Si−O−Si bond angle affect the Si−Si distances but excludes any effect of libration. The three graphs show those vectors with their largest components parallel to the three crystallographic axes *a*, *b*, and *c*. The keys list *Pnnm* labels first and *Immm* labels second.

the silicon resonances into two groups of two and three atoms, respectively. $\cos(\alpha)/(\cos(\alpha) - 1)$ curves for Si2, Si4, and Si3 cross just below the transition temperature, as do the $\cos(\alpha)/(\cos(\alpha) - 1)$ curves for Si5 and Si1. This behavior is matched almost exactly by the chemical shift curves, the Si2, Si4, and Si3 resonances almost coalescing between 300 and 350 K, and the Si5 and Si1 resonances coalescing at about the same temperature. The results from the single-crystal structure are therefore perfectly consistent with the MAS NMR spectra, and the seemingly higher symmetry spectra collected at ∼300−350 K are due not to an increase in symmetry but simply to differing accidental overlap of the resonances as a function of temperature.

While the trends in the two curves in Figure 6 are very similar, it is interesting to note that there are some significant differences. The *relative* slopes of the curves are similar in the two cases, but the *absolute* slopes are markedly different. For example, Si1, Si4, and Si3 show a sharp change in behavior in the $\cos(\alpha)/(\cos(\alpha) - 1)$ curve between 150 and 350 K, but show very little change in chemical shift over the same temperature range. The opposite effect is shown by Si2 and Si5, almost no change in the $\cos(\alpha)/(\cos(\alpha) - 1)$ curve but a relatively large change in chemical shift. Such differences in behavior are perhaps not surprising given the relatively simple nature of the geometric function that is used. While we do not currently have NMR spectra of the high-temperature form of ferrierite, the $\cos(\alpha)/(\cos(\alpha) - 1)$ curve would indicate that we should expect to see the four resonances split into three groups. Si2 and Si4 should be well resolved with Si4 at the lowest field. Si1 and Si3 should give resonances at the highest field with similar chemical shifts, and Si2 should have a chemical shift intermediate between the two extremes. It will be very instructive to see

whether the $\cos(\alpha)/(\cos(\alpha) - 1)$ curve can be used in such a way to predict the approximate NMR spectrum of the high-temperature phase.

Of course the most important feature of the changes in atomic positions, at least with regard to any application of the materials, is the effect this has on the size and shape of the pores in the zeolite. The move to higher symmetry affects both the 8- and 10-membered pore openings by quite a large amount. At low temperatures both pore openings are wider at one end than they are at the other (i.e., the pore openings are "egg" shaped), while at the higher temperature they become a more symmetrical "oval" shape. Interestingly, because of the shape of the thermal expansivity curve (Figure 2), there are two temperatures at which the unit cell volume of FER has the same value. However, the shape of the pores will be subtly different in each case. In principle, this could lead to some interesting temperature-dependent adsorption properties, although, since this is quite a small effect, it is most likely of limited interest for applications. In addition, the adsorption properties of the material will be affected markedly by the vibrations (e.g., breathing of the pores), and this will also have an effect since the amplitude of vibrations will certainly be greater at higher temperatures.

From Figure 2 it is clear that the overall thermal expansion of the low-temperature *Pnnm* form of FER is anisotropic; the unit cell size increases in two dimensions but decreases in the third. This can be explained by considering the competing changes in Si−O−Si bond angles and transverse vibrations that are occurring.

Figure 7 shows three graphs of the changes in Si−Si distance caused by a change in the respective Si−O−Si bond angle. This calculated Si−Si distance takes no account of the effect of transverse vibrations. The three graphs show the Si−Si distances

Table 1. Angles, θ, and cos θ Made between Each of the Si(O)Si Vectors in the *Immm* FER Structure and the Three Crystallographic Axes[a]

Si–Si vector (*Pnnm*)	θ_a	θ_b	θ_c	cos θ_a	cos θ_b	cos θ_c	Si–Si vector (*Immm*)
Si1(O8)Si2	0.00	90.00	90.00	1.00	0.00	0.00	Si2(O1)Si2
Si2(O3)Si5	77.84	22.20	71.73	0.21	0.92	0.31	Si4(O2)Si2
Si3(O1)Si3	90.00	90.00	0.00	0.00	0.00	1.00	Si1(O3)Si1
Si5(O2)Si5	0.00	90.00	90.00	1.00	0.00	0.00	Si4(O4)Si4
Si1(O6)Si3	45.24	63.84	56.18	0.70	0.44	0.55	Si1(O5)Si2
Si3(O4)Si4	90.00	24.97	65.03	0.00	0.90	0.42	Si1(O6)Si3
Si4(O10)Si5	45.73	90.00	44.27	0.69	0.00	0.71	Si3(O7)Si4
Si2(O9)Si1	78.21	64.83	28.15	0.20	0.43	0.88	Si2(O8)Si2

[a] cos θ can be used as a measure of how much a change in the Si−Si distance would contribute to a change in the magnitude of the respective crystallographic axes.

that are most important to the three unit cell axes; i.e., only those Si−Si distances whose interatomic vector has its major component parallel to the axis in question are shown on the graph for that axis. It should be remembered that a change in any of the Si−Si distances will in general affect each of the three axes to some degree, depending on the orientation of the Si−Si vector relative to the unit cell axis in question. Table 1 lists the relative orientations of each Si(O)Si interatomic vector and the angle, θ, it makes with each of the three crystallographic axes for the *Immm* structrue. The orientations of the equivalent vectors in the *Pnnm* structure vary only slightly from these. cos θ can be used as a measure of how much a change in the Si−Si distance would contribute to a change in the magnitude of the respective crystallographic axes; if cos θ is greater than ∼0.7 (i.e., $\theta <$ ∼45°) a change in that particular Si(O)Si bond angle can be said to strongly contribute to a change in that axis.

Let us consider first the thermal behavior of FER below the phase transition, where the structure is still *Pnnm* (so the bond angle labeling refers to the *Pnnm* column in Table 1). Five Si−Si distances can be identified as having their major component parallel to the a axis. One of these, the Si1−(O6)−Si3 distance, strongly increases by more than 0.1 Å over the temperature range, while one, the Si2−(O7)−Si3 distance, decreases, but not by quite as much. The other three all increase slightly or show no significant change. Overall, the expansion caused by the large change in the Si1−O6−Si3 angle dominates, and the a axis unit cell length increases with temperature.

Three Si−Si interatomic vectors can be identified as having their major component parallel to the b axis. The changes to these three distances are smaller, two increasing slightly and one decreasing slightly. Overall one might then expect a slight increase in this direction. However, the transverse vibrations that exist for all three of the Si−O−Si angles must outweigh the changes in these angles and lead to a very slight overall decrease in this direction. The two Si−Si distances that will effect the biggest change in the c axis are Si2−Si1 (connected through O9) and Si3−Si3 (connected through O1). Both these interatomic vectors are aligned almost parallel with the c axis, and increase significantly over the temperature range, leading to a relatively marked increase in the c axis length. These two bond angle changes dominate in this direction.

Above the phase transition temperature (*Immm* structure) the contraction of the three crystallographic axes is much more isotropic than the expansion, with the c axis contracting only slightly more than the other two axes. The extent of the contraction must be correlated with the magnitude of transverse

vibrations, which is in turn related to the atomic displacement parameters (ADPs or temperature factors) of the oxygen atoms as measured by X-ray diffraction. Unfortunately, while atomic positions are relatively unaffected by the lower precision of the refinements at high temperatures, the ADPs will be affected to a greater degree, so any correlation between the ADPs and transverse vibrations must be regarded as qualitative. However, by comparing the magnitudes of the equivalent isotropic displacement parameters (U_{equiv}), we can at least get some idea of the atoms that are important in the NTE. Once again we can identify the extent to which each change in these atoms affects the various crystallographic axes from Table 1. The larger contraction in the c axis is relatively easy to rationalize from these temperature factors. The oxygen that takes part in the constrained 180° bond angle in *Immm*, O8 (the numbering scheme in this section refers to the *Immm* structure), shows a strong change above the phase transition, and has a large U_{equiv}. This is consistent with the motion of the oxygen atom changing at the phase transition temperature so that it undergoes a toroidal motion around the Si2−Si2 interatomic vector in the high-temperature phase, a situation that is often used to explain such 180° bond angles. The next largest U_{equiv} belongs to O7, and the strong transverse vibration of this oxygen will also lead to strong contraction along the c axis. It is surprising that O3 has a relatively small U_{equiv} value at high temperatures, as it is the oxygen that links the layers in the structure together, so one might expect it to have more easily excited transverse vibrations than oxygen atoms that are held in the layers. This may in fact be the case as O3 shows the most anisotropic displacement parameters of all the oxygen atoms with transverse components of magnitudes similar to those of O7 and O8 but with the parallel component being significantly smaller than those of all the other atoms, leading to a small U_{equiv} value. Therefore, it would appear that transverse vibrations of O3, O7, and O8 are the most important in explaining the larger NTE of the *Immm* phase parallel to the c axis.

All the oxygen atoms that contribute to the contraction of the a and b axes seem to vibrate with approximately the same amplitude as they all have similar U_{equiv} values. These are significantly smaller than O7 and O8 and are not as anisotropic as O3, so the amplitude of the transverse vibrations will be smaller, leading to less contraction in this layer. Overall, this fits well with our expectations, as it is likely that the most inflexible part of the structure will be the fairly dense layers, with the most flexible regions being those perpendicular to the layers.

The overall effect of the changes in Si−O−Si bond angles below the transition temperature is that the SiO$_4$ tetrahedra "unfold" toward a maximum volume. At this point, the Si−O−Si bond angles can no longer increase (i.e., the SiO$_4$ tetrahedra are no longer unfolding outward). Above the phase transition temperature the RUMs or qRUMs are still the dominant low-energy vibrational modes in the structure (in fact, calculations show that there will be more RUMs in high-symmetry structures compared to low-symmetry ones[16]). However, the situation is somewhat different in that the magnitude of the Si−O−Si angles does not now increase, and therefore does not contribute to any increases in Si−Si distances as happens in the low-symmetry structure. The transverse vibrations are still present, and act to reduce the average Si−Si

distance, leading to a reduction in the length of all three crystallographic axes and therefore to overall negative thermal expansion. The RUMS are, in essence, cooperative rotations of the tetrahedra in the structure, and lead to a slight "collapse" of the walls of the structure into the pores. This reduces the amount of space taken up by the structure as a whole, and leads to overall contraction.

The variable-temperature ^{29}Si NMR spectra of zeolite IFR[6] show no changes in chemical shift with temperature, consistent with the Si−O−Si bond angles remaining constant throughout the experiment. Since a similar situation is seen for FER in this work for its high-temperature form, it may well be that the chemical shifts for the *Immm* phase will also be invariant.

It is now clearly established that the siliceous form of zeolite FER undergoes a displacive phase transition at around 400 K. Below this phase transition the material exhibits positive thermal expansion, driven by changes in Si−O−Si bond angles as the maximum topological symmetry of the structure is approached. Above the phase transition the material changes thermal behavior quite drastically, exhibiting strongly negative thermal expansion. However, this is not driven by changes in crystallographically determined average Si−O−Si bond angles but by cooperative rotations of all tetrahedra driven by rigid unit modes of vibration, while these individual Si−O−Si angles are kept essentially constant throughout the contraction. From accurate powder and single-crystal X-ray diffraction experiments we have successfully modeled these changes in the average atomic positions in the structure with temperature and shown that these changes can be correlated with changes seen in the magic angle spinning NMR experiments. This work illustrates the scope of variable-temperature X-ray diffraction experiments in elucidating the changes that occur in what are usually thought of as dynamic processes induced by thermal vibration of the frameworks as a whole. Accurate single-crystal X-ray diffraction studies as the processes involved develop with temperature also provide excellent benchmark data with which results from calculations, such as those based on rigid unit mode theory, can be compared.

Supporting Information Available: Crystallographic information files (CIFs) for single-crystal X-ray studies. This material is available free of charge via the Internet at http://pubs.acs.org.

JA0292400